

# Imaging features of primary hepatic leiomyosarcoma: A case report and review of literature

WEI-FU LV<sup>1,2</sup>, JIAN-KUI HAN<sup>1</sup>, DE-LEI CHENG<sup>2</sup>, WEN-JING TANG<sup>2</sup> and DONG LU<sup>2</sup>

<sup>1</sup>Positron Emission Tomography/Computed Tomography Center, Qilu Hospital, First Affiliated Hospital of Shandong University, Jinan, Shandong 250012; <sup>2</sup>Department of Radiology, Affiliated Anhui Provincial Hospital of Anhui Medical University, Hefei, Anhui 230001, P.R. China

Received June 6, 2014; Accepted February 10, 2015

DOI: 10.3892/ol.2015.3006

**Abstract.** Primary hepatic leiomyosarcoma (PHL) is an extremely rare tumour. This tumour is difficult to diagnose by imaging examinations due to its rarity, and non-specific conventional imaging manifestations and clinical presentation. The present study reports the case of a 42-year-old male with PHL that was confirmed by histopathological and immunohistochemical examinations. Multimodal imaging examinations, including ultrasound, computed tomography (CT), magnetic resonance imaging (MRI), positron emission tomography-CT and digital subtraction angiography, were performed. The imaging manifestations were analysed and the associated literature was reviewed. The results found that no characteristic imaging appearance was present on ultrasound or plain CT scan. However, on unenhanced MRI, the tumours presented with a heterogeneous low signal density on T1-weighted imaging (WI) and a high signal density on T2WI and diffusion-WI. On gadopentetate dimeglumine enhanced MRI, the lesions were not enhanced during the arterial and portal venous phases; by contrast, these lesions were evidently enhanced during the 5-min delayed phase. Therefore, the delayed imaging of enhanced MRI is likely to be used to differentiate PHL from other hepatic tumours.

## Introduction

Primary hepatic leiomyosarcoma (PHL) is an exceedingly rare tumour. In total, <50 patients with PHL were reported in the English literature up until 2011. Among these patients, only five cases were involved in radiological studies (1-5). PHL may develop from the smooth muscle cells of intra-hepatic vascular structures, bile ducts or ligamentum

teres (1,3). It is difficult to obtain an early diagnosis due to the rarity, and non-specific conventional imaging manifestations and clinical presentation (6). Imaging examinations play a significant role in detecting and differentiating the hepatic masses (7). The present study reports the case of a middle-aged male with PHL. The patient was subjected to multimodal imaging examinations, including ultrasound, computed tomography (CT), magnetic resonance imaging (MRI), positron emission tomography-CT (PET-CT) and digital subtraction angiography (DSA). The imaging manifestations were analysed and the associated literature was reviewed.

## Case report

In July 2013, a 42-year-old male presented to the First Affiliated Hospital of Shandong University (Jinan, China) with abdominal pain, marasmus and weakness that had persisted for two months. A physical examination revealed a notable hepatomegaly extending ~3 cm below the right costal margin. The patient had no medical history of previous liver diseases or alcohol abuse. Laboratory analysis showed normal liver and kidney functions. Other laboratory tests, including red blood cell, white blood cell and platelet counts, and hepatitis B surface antigen, hepatitis C virus antibody,  $\alpha$ -fetoprotein, carbohydrate antigen 19-9 and carcinoembryonic antigen analysis, were normal.

Abdominal ultrasonography (ClearVue 350; Philips Medical Systems, Best, the Netherlands) revealed two well-defined heterogeneous hypoechoic masses in the caudate lobe and the left lobe of the liver. The sizes of the two masses were 9.1x7.4x6.6 and 3.8x3.5x3.8 cm, respectively (Fig. 1).

A plain CT (Discovery CT750 HD; GE Medical Systems Ltd., Milwaukee, WI, USA) scan disclosed two slight hypodense lesions with a definite margin, arising from the caudate lobe and the left lobe of the liver. Moreover, multiple hypodense lesions around the two larger lesions were observed. The inferior vena cava was compressed by the mass of the caudate lobe, but no enlarged lymph nodes were found (Fig. 2).

MRI was performed using a 3.0 Tesla whole-body MR hybrid system (Trio Time, Siemens, Germany) with regular pulse sequences. T1-weighted imaging (WI),

---

*Correspondence to:* Professor Jian-Kui Han, Positron Emission Tomography/Computed Tomography Center, Qilu Hospital, First Affiliated Hospital of Shandong University, 107 Cultural West Road, Jinan, Shandong 250012, P.R. China  
E-mail: jiankuihan99@163.com

**Key words:** primary hepatic leiomyosarcoma, liver, imageology, smooth muscle actin

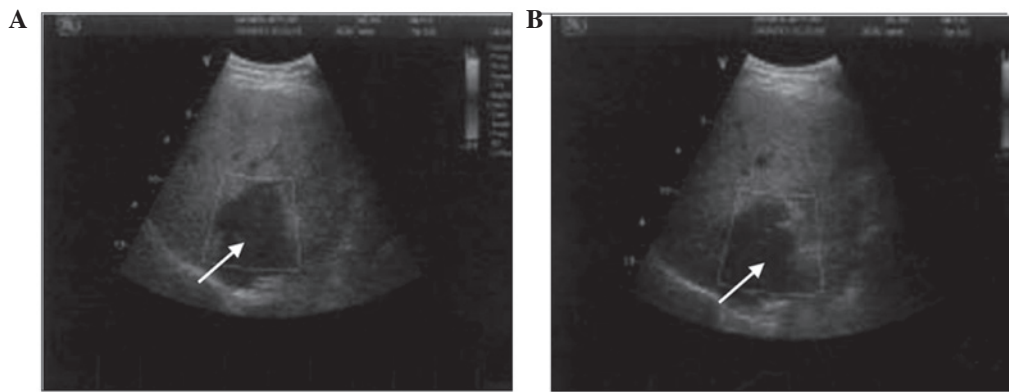


Figure 1. Ultrasound findings of primary liver leiomyosarcoma. (A) Two dimensional scanning showing a large heterogeneous hypoechoic mass (white arrow) in the caudate lobe of the liver. (B) Doppler flow imaging showing no blood flow signal.

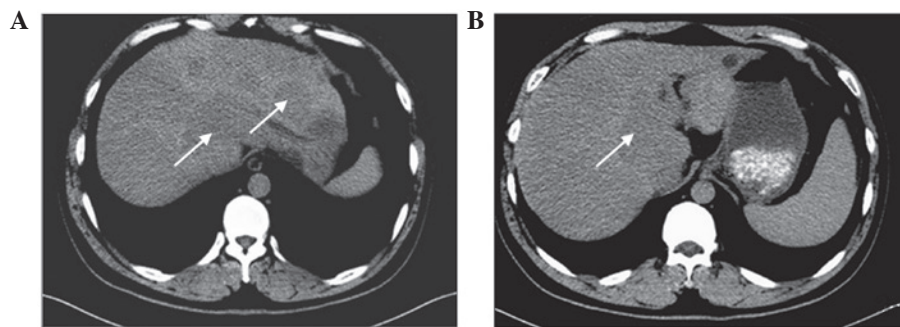


Figure 2. Computed tomography (CT) findings of primary liver leiomyosarcoma. (A) Plain CT showing slightly low-density lesions (white arrow) with definite borders in the caudate and left lobes of the liver. (B) lower scan slice revealing a definite tumour border.

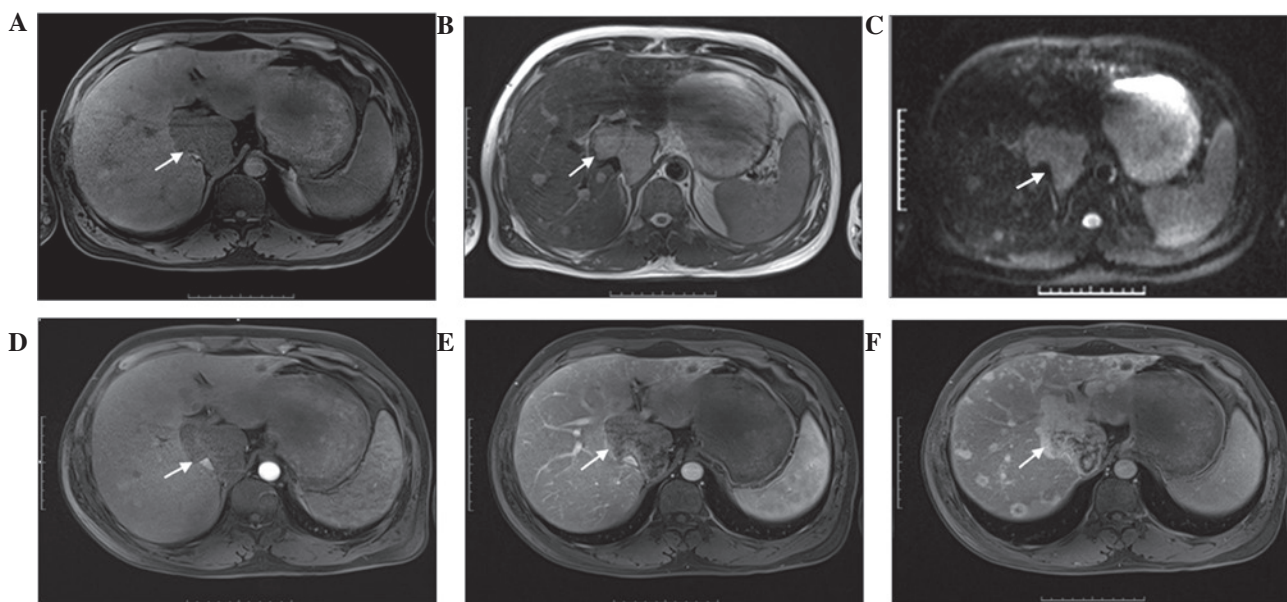


Figure 3. MRI findings of primary liver leiomyosarcoma. (A) On T1-weighted imaging (WI), the masses (white arrow) are well defined and slightly heterogeneous hypointensities. (B) On T2WI, the masses (white arrow) are heterogeneous hyperintensities. (C) On diffusion-WI, the masses (white arrow) display hyperintensity. (D) In the arterial phase of dynamic contrast-enhanced imaging, the masses (white arrow) show no enhancement. (E) In the venous phase of dynamic contrast-enhanced image, no evident enhancement can be observed. (F) In the 5-min delayed imaging, the majority of areas of the mass (white arrow) show marked enhancement. The intrahepatic metastases are also enhanced.

T2WI, diffusion-WI (DWI) and gadopentetate dimeglumine-enhanced dynamic MRI were performed. The tumours presented with a heterogeneous low signal density on T1WI

(Fig. 3A) and a high signal density on T2WI (Fig. 3B). Furthermore, these tumours exhibited well-defined margins, but no evident capsule was observed. Satellite lesions were clearly

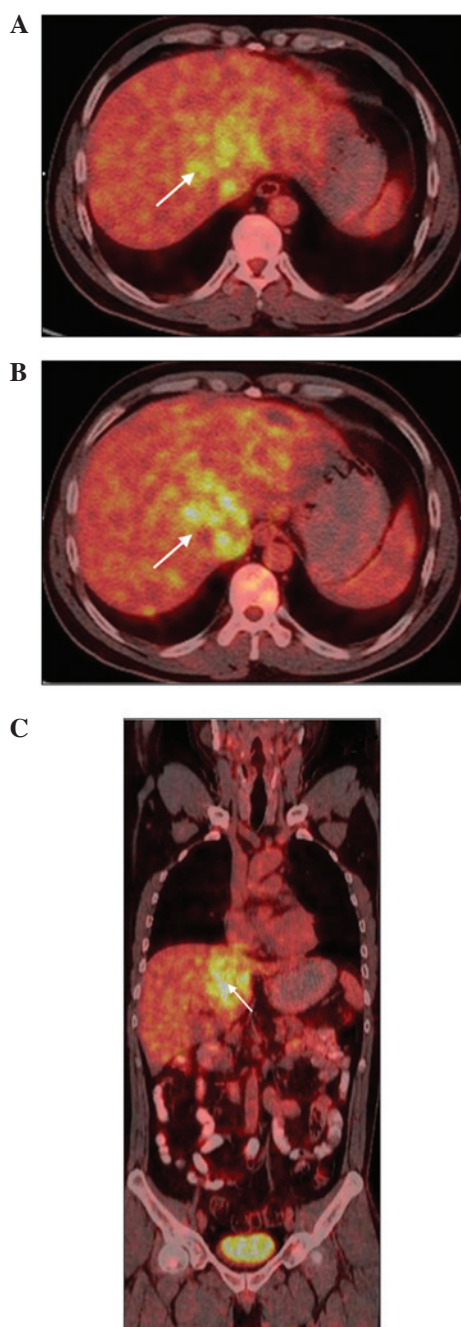


Figure 4.  $^{18}\text{F}$ -fluorodeoxyglucose (FDG) positron emission tomography-computed tomography (PET-CT) findings of primary liver leiomyosarcoma. (A) PET-CT shows higher  $^{18}\text{F}$ -FDG uptake lesions on the liver (white arrow), corresponding to the tumour revealed by CT and MRI. (B) On the lower scan slice, multiple intrahepatic metastases are observed (white arrow). (C) On the whole body scan, no evidence of remote metastases is observed.

shown on T2WI and DWI (Fig. 3B and C). On enhanced MRI (Fig. 3D-F), the lesions were not enhanced during the arterial and portal venous phases; by contrast, these lesions were evidently enhanced during the 5-min delayed phase.

A whole body PET-CT (Biograph 16; Siemens Healthcare, Erlangen, Germany) scan was conducted to detect the masses and determine whether they were primary or metastatic. The scan spanned the base of the skull to the upper thighs. PET-CT showed multiple increased FDG uptake lesions in the liver; such lesions corresponded to the tumours revealed by CT

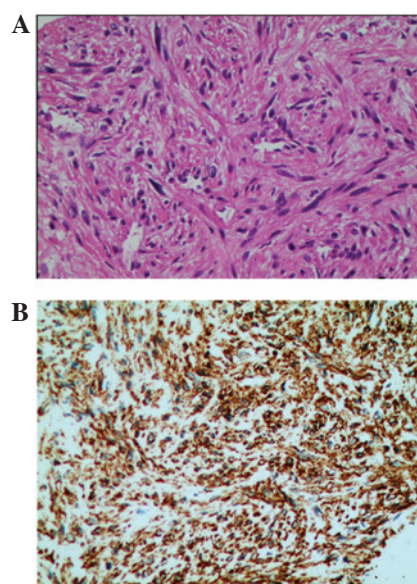


Figure 5. Pathological findings of primary liver leiomyosarcoma. (A) Haematoxylin and eosin staining showing the proliferation of spindle cells, with hyperchromatic pleomorphic nuclei and eosinophilic cytoplasm, arranged in crosswise bundles (magnification, x400). (B) Immunohistochemical staining revealing tumour cells positive for smooth muscle actin (magnification, x400).

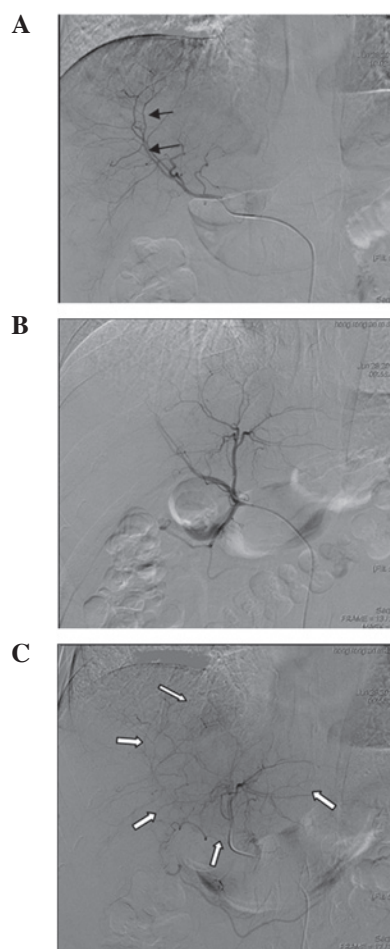


Figure 6. Digital subtraction angiography findings of primary liver leiomyosarcoma. (A) Selective angiography of the hepatic artery shows no tumour stain in the caudate lobe, however compression and displacement of the vessel branches is observed (black arrow). (B) In the arterial phase of super-selective angiography, no obvious tumour stain is observed. (C) In the delayed phase, a weak tumour stain is observed (white arrows).

and MRI. No evidence of metastasis from other organs was observed (Fig. 4).

On the basis of the findings, a specific type of hepatic malignant tumour was suspected. This tumour was then subjected to CT-guided transcutaneous puncture biopsy. Microscopic examination showed that the tumour was characterised by intersecting bundles of spindle-shaped cells, with eosinophilic cytoplasm and nuclear atypia. Immunohistochemical staining revealed that the tumour cells were positive for smooth muscle actin (SMA; Fig. 5) and desmin; by contrast, these tumour cells were negative for c-Kit (CD117), discovered on gastrointestinal stromal tumours 1 (DOG1), human melanoma black 45 (HMB45), PNL2 and Ki-67. These findings indicated the occurrence of PHL.

DSA (Innova 3100 system; GE Healthcare, Waukesha, WI, USA) of the hepatic artery was performed to administer chemotherapeutic drugs via transcatheter arterial infusion due to the loss of surgical removal indications. DSA showed that the branches of the hepatic artery that passed into the caudate lobe were slightly increased and depressed. No tumour stain was found during the arterial and portal venous phases, whereas weak stain was detected during the delayed phase (Fig. 6).

The patient underwent transarterial infusion (TAI) with 60 mg epirubicin and 800 mg carboplatin on day 1. On the second day, the patient received a 24 h intravenous infusion of 5 g/m<sup>2</sup> ifosfamide and 5 g/m<sup>2</sup> mesna. An additional 24 h infusion of 2 g/m<sup>2</sup> mesna was administered on day 3. One cycle lasted for 7 days and a total of four cycles of treatment were administered over a period of four months. Follow-up examination eight months after the initiation of TAI treatment revealed that the tumours had stabilized, according to the modified Response Evaluation Criteria in Solid Tumors guidelines (8). However, the patient succumbed to liver failure 384 days after the initiation of TAI treatment.

The present case report was approved by the Ethics Committee of the First Affiliated Hospital of Shandong University and written informed consent was obtained from the patient for publication of the case report and any accompanying images.

## Discussion

The clinical manifestations of PHL are non-specific, and tumours are generally asymptomatic until they increase in size (9-11). Abdominal pain, weight loss, vomiting and jaundice are the common symptoms, while hepatomegaly and a palpable mass are frequently disclosed on physical examination. Acute bleeding is a rare symptom observed in patients with PHL (12). Liver function test results may be abnormal, but serological markers, such as  $\alpha$ -fetoprotein, are normal. The absence of serological markers and non-specific clinical manifestations often delay diagnosis (2,7).

The CT findings of PHL reveal a large, well-defined and heterogeneous hypodensity mass with internal and peripheral enhancement (13), or a cystic mass with an enhanced thickened wall (1,14). In the present case, the plain CT scan showed two well-defined masses with heterogeneous hypodensity in the caudate lobe and the left lobe of the liver; multiple satellite lesions were also observed in the remaining portion of the liver. These findings are similar to those recorded in previously

reported studies (1-4). However, an enhanced CT scan was not performed in the present case.

Soyer *et al* (5) reported the case of one patient with PHL who was subjected to MRI; the results showed that the tumours exhibited homogeneous or heterogeneous hypointensity in T1WI and hyperintensity in T2WI with occasional encapsulation. Similar MRI characteristics are also observed in the present case. In previous studies, the patients were subjected to unenhanced MRI. However, complete MRI sequences, including unenhanced MRI, DWI and dynamic contrast-enhanced MRI, were performed in the present case. The tumours in DWI showed hyperintensity, suggesting a limited diffusion of water molecules in the tumour. In the dynamic contrast-enhanced MRI, the masses were not evidently enhanced during the arterial and portal venous phases. However, the masses were markedly enhanced during the 5-min delayed imaging. This result could be a specific MRI characteristic of PHL.

No tumour stain was found during the arterial and portal venous phases, whereas weak stain was detected during the delayed phase of DSA. These findings are consistent with those of the enhanced MRI. Furthermore, these results could be used to differentiate PHL from hepatocellular carcinoma and liver haemangioma.

PET-CT can be applied to sensitively detect primary tumours and metastases. In the present case, multiple masses were found in the liver, with increased FDG metabolism. No lesions were detected in the other organs. Therefore, hepatic metastases could be excluded.

The histopathological diagnosis of PHL is characterised by the presence of uniform and diffuse infiltrates of spindle-shaped cells with hyperchromatic nuclei; the diagnosis is further confirmed by a positive immunohistochemistry reaction for SMA, desmin and vimentin, as well as a negative reaction for keratin and S-100 protein (15,16). In the present case, a microscopic examination showed intersecting bundles of spindle-shaped cells with eosinophilic cytoplasm and nuclear atypia. Moreover, immunohistochemistry revealed a positive reaction for SMA and desmin, and a negative reaction for c-kit receptor (CD117), DOG1, HMB45, PNL2 and Ki-67. Therefore, the diagnosis of PHL was confirmed.

In conclusion, in the present study, PHL was found to be a hypovascular tumour, which was not evidently enhanced during the arterial and portal venous phases on MRI, and exhibited no tumour stain on DSA. However, the lesions were evidently enhanced during the delayed imaging of enhanced MRI. These findings may reveal the imaging characteristics of PHL, however, further studies are required to confirm this. The microscopic characteristics of PHL included intersecting bundles of spindle-shaped cells with eosinophilic cytoplasm and nuclear atypia. Immunohistochemistry revealed a positive reaction for SMA, desmin, and vimentin.

## References

1. Ferrozzi F, Bova D, Zangrandi A and Garlaschi G: Primary liver leiomyosarcoma: CT appearance. *Abdom Imaging* 21: 157-160, 1996.
2. Shamseddine A, Faraj W, Mukherji D, *et al*: Unusually young age distribution of primary hepatic leiomyosarcoma: case series and review of the adult literature. *World J Surg Oncol* 8: 56, 2010.

3. Civardi G, Cavanna L, Iovine E, *et al*: Diagnostic imaging of primary hepatic leiomyosarcoma: a case report. *Ital J Gastroenterol* 28: 98-101, 1996.
4. Gandhi MR, Wong DC and Wood DJ: Ultrasound and computed tomography appearances of primary hepatic leiomyosarcoma. *Australas Radiol* 39: 289-291, 1995.
5. Soyer P, Blanc F, Vissuzaine C, *et al*: Primary leiomyosarcoma of the liver MR findings. *Clin Imaging* 20: 273-275, 1996.
6. Chi M, Dudek AZ and Wind KP: Primary hepatic leiomyosarcoma in adults: analysis of prognostic factors. *Onkologie* 35: 210-214, 2012.
7. Tsai PS, Yeh TC and Shih SL: Primary hepatic leiomyosarcoma in a 5-month-old female infant. *Acta Radiol Short Rep* 2: 2047981613498722, 2013.
8. Lencioni R and Llovet JM: Modified RECIST (mRECIST) assessment for hepatocellular carcinoma. *Semin Liver Dis* 30: 52-60, 2010.
9. Holloway H, Walsh CB, Thomas R and Fielding J: Primary hepatic leiomyosarcoma. *J Clin Gastroenterol* 23: 131-133, 1996.
10. Rosas JS, Del Rosario A, Bui HX, *et al*: Primary hepatic leiomyosarcoma in a child with the acquired immunodeficiency syndrome. *Hum Pathol* 23: 69-72, 1992.
11. Brichard B, Smets F, Sokal E, *et al*: Unusual evolution of an Epstein-Barr virus-associated leiomyosarcoma occurring after liver transplantation. *Pediatr Transplant* 5: 365-369, 2001.
12. Jeong TY, Kim YS, Park KJ, *et al*: A case of primary leiomyosarcoma of the liver presenting with acute bleeding. *Korean J Gastroenterol* 51: 194-198, 2008 (Korean).
13. Gates LK Jr, Cameron AJ, Nagorney DM, *et al*: Primary leiomyosarcoma of the liver mimicking liver abscess. *Am J Gastroenterol* 90: 649-652, 1995.
14. Yu RS, Chen Y, Jiang B, *et al*: Primary hepatic sarcomas: CT findings. *Eur Radiol* 18: 2196-2205, 2008.
15. Smith MB, Silverman JF, Raab SS, *et al*: Fine-needle aspiration cytology of hepatic leiomyosarcoma. *Diagn Cytopathol* 11: 321-327, 1994.
16. Sprogø-Jakobsen S and Hølund B: Immunohistochemistry (Ki-67 and p53) as a tool in determining malignancy in smooth muscle neoplasms (exemplified by a myxoid leiomyosarcoma of the uterus). *APMIS* 104: 705-708, 1996.